Study of the Water–Gas–Shift Reaction on Pd@CeO 2 /Al 2 O 3 Core–Shell Catalysts †

ARTICLE *in* THE JOURNAL OF PHYSICAL CHEMISTRY C · JUNE 2010

Impact Factor: 4.77 · DOI: 10.1021/jp102965e

Study of the Water-Gas-Shift Reaction on $Pd@CeO_2/Al_2O_3$ Core−Shell Catalysts†

Noah L. Wieder,‡ Matteo Cargnello,§ Kevin Bakhmutsky,‡ Tiziano Montini,§ Paolo Fornasiero,*,§ and Raymond J. Gorte*,‡

Department of Chemical and Biomolecular Engineering, University of Pennsylvania, 311A Towne Building, 220 South 33rd Street, Philadelphia, Pennsylvania 19104, and Chemistry Department, ICCOM-CNR, INSTM, Center of Excellence for Nanostructured Materials (CENMAT), University of Trieste, Via L. Giorgieri 1, 34127 Trieste, Italy

Received: April 1, 2010; Revised Manuscript Received: May 26, 2010

An alumina-supported, $Pd@CeO_2$, core−shell catalyst having 1 wt % Pd and 9 wt % ceria was characterized for the water-gas-shift (WGS) reaction. Although the catalyst initially exhibited similar WGS rates to that of a conventional Pd/ceria catalyst at 623 K in 25 Torr each of CO and H_2O, the $Pd@CeO_2$ catalyst deactivated severely over the period of 1 h. The WGS activity of the $Pd@CeO_2$ could be completely restored by mild oxidation, and oxygen-titration measurements showed that the ceria shell in the $Pd@CeO_2$ catalyst was significantly reduced after being used for the WGS reaction. These observations are in sharp contrast to those found with a conventional Pd/ceria catalyst, for which the ceria remains almost fully oxidized under WGS conditions. CO adsorption measurements, using FTIR at room temperature and CO uptakes at 195 K, indicated that Pd in the oxidized $Pd@CeO_2$ catalyst was accessible to CO, but adsorption was completely suppressed on the reduced catalyst. A model is presented to explain the results, which assumes that cracks and fissures in the oxidized ceria shell allow access to the Pd core but that reduction blocks access, either due to changes in the density of the ceria, which closes the fissures, or to coverage of the metal surface with ceria.

1. Introduction

Interactions between catalytic metals and their supports can have a large influence on activity. For example, reaction rates for the water-gas-shift (WGS) reaction on ceria-supported Pd has been shown to be orders of magnitude larger than WGS rates on either ceria or Pd-alumina, implying that contact between the Pd and the ceria is crucial for achieving high rates in this system.[1] Indeed, ceria-supported metals exhibit higher activities than metals on other supports for a number of reactions,[2] due in large part to the ease with which Ce is able to shuttle between its III and IV oxidation states. However, ceria-supported metals are prone to sintering under WGS conditions, with the resulting loss of catalytic activity.[3,4] A possible approach to preventing metal sintering is to embed isolated metal particles inside a porous shell of the oxide. This strategy has been used by Corma and co-workers, who reported that catalysts formed by encapsulated Au and Pd nanoparticles in SiO_2 were active and stable.[5,6] Others have also reported novel catalytic properties for metal catalysts embedded in oxide supports.[7,8]

Our groups have recently demonstrated enhanced stability for ceria-encapsulated Pd for the WGS reaction;[9] however, because the catalysts were prepared by a microemulsion procedure, it was difficult to control both the Pd particle size and the shell thickness. Therefore, the Pd-ceria catalysts exhibited relatively low activities, probably due to diffusion limitations through the ceria shell.[9] To avoid this problem, we have developed an alternative approach to preparing $Pd@CeO_2$ catalysts that provides more flexibility for tuning both the Pd core size and the ceria shell thickness.[10] These $Pd@CeO_2$ nanostructures are dispersible in organic solvents and are easily deposited onto supports such as alumina. In our previous work, we demonstrated that catalysts prepared in this way show high activity for the CO-oxidation, WGS, and methanol-steam-reforming reactions.

In the present paper, we demonstrate that the alumina-supported, $Pd@CeO_2$ catalysts exhibit unusual catalytic properties under WGS reaction conditions. Unlike bulk ceria,[11] the ceria shell in these catalysts undergoes significant reduction in the WGS reaction environment. Although CO is able to adsorb on the Pd core of the oxidized catalyst, the reduced $Pd@CeO_2/Al_2O_3$ catalysts do not adsorb CO, so that these catalysts lose activity for the WGS reaction as they undergo reduction. The results of this study have implications for the development of more active and stable catalysts through the manipulation of nanostructure.

2. Experimental Methods

$Pd@CeO_2$ particles were prepared according to the procedure reported elsewhere.[10] Briefly, $Pd@CeO_2$ was obtained by reacting preformed 11-mercaptoundecanoic acid-protected Pd nanoparticles with a cerium(IV) alkoxide, followed by a controlled hydrolysis in the presence of dodecanoic acid. After dissolving the $Pd@CeO_2$ particles in THF, the alumina (Sasol), which had been degassed at 500 K overnight, was added to the solution. This solution was stirred overnight before removing the THF by evacuation. Finally, the resulting powder was calcined at 773 K for 5 h using a heating ramp of 3 K/min. The composition of the material was 1 wt % Pd and 9 wt % ceria. For comparison purposes, experiments were also conducted on a conventional 1% Pd/ceria catalyst. The conventional sample was made by wet impregnation of $Pd(NO_3)_2$ solution onto ceria that had been prepared by decomposition of $Ce(NO_3)_3 \cdot 6H_2O$.

† Part of the "Alfons Baiker Festschrift".

* To whom correspondence should be addressed. E-mail: gorte@seas.upenn.edu; pfornasiero@units.it.

‡ University of Pennsylvania.

§ University of Trieste.

10.1021/jp102965e
Published on Web 06/21/2010

The surface area of this sample was 67 m^2/g; other characteristics are described elsewhere.[12]

WGS rates were measured in a tubular reactor at atmospheric pressure, using partial pressures of 25 Torr each for CO and H_2O. Rates were reproduced several times, using catalyst-sample sizes between 0.08 and 0.2 g. Water was introduced to the reactor by saturation of a He carrier gas flowing through a deionized water saturator, and the partial pressures of CO, H_2O, and He were controlled by adjusting the relative flow rates of each component. The total flow rate of gas was maintained at 150 mL/min. The conversions of CO and H_2O were kept below 10% so that differential conditions could be assumed. The composition of the effluent from the reactor was monitored using an online gas chromatograph, SRI8610C, equipped with a Hayesep Q column and a TCD detector.

BET isotherms were measured using N_2 on a Micromeritics ASAP 2020C. The samples were first degassed in vacuum at 625 K overnight prior to N_2 adsorption at liquid nitrogen temperature. Powder X-ray diffraction patterns were collected on a Philips PW 1710/01 instrument with Cu Kα radiation (graphite monochromator). Diffraction patterns were taken with a 0.02° step size, using a counting time of 10 s per point.

Because exposure of a conventional, oxidized Pd/ceria catalyst to CO at room temperature can cause reduction of the ceria and adsorption of the resulting CO_2 onto the reduced ceria in the form of a carbonate,[13,14] two different protocols were used to measure CO chemisorption properties of these catalysts. These two protocols allowed the measurement of CO adsorption on a reduced sample and an oxidized sample. To measure CO adsorption on the reduced sample, the catalyst was first prereduced in H_2 at 673 K, after which the CO adsorption uptake was measured at room temperature. To measure CO adsorption on the oxidized sample, CO adsorption was measured at 195 K, a temperature that has been reported to be sufficiently low to prevent reduction of ceria-supported catalysts by CO.[15] For this second protocol, the catalyst was first oxidized at 673 K in 200 Torr O_2 for several minutes, evacuated, and then reoxidized and evacuated several times. Next, the sample was cooled to 423 K and exposed to 200 Torr H_2 for several minutes to reduce the PdO to Pd. After evacuation, the CO uptake was measured at 195 K by adding small pulses of CO until a rise in the pressure of the sample cell was detected.

FTIR spectra were recorded using a Mattson Galaxy 2020 FTIR spectrometer equipped with a Spectra-Tech Collector II diffuse-reflectance accessory. A controlled atmosphere sample chamber allowed the FTIR experiments to be performed under various flow and temperature conditions. Infrared spectra of the $Pd@CeO_2/Al_2O_3$ catalysts were measured on both oxidized and reduced samples. To produce the reduced sample, the catalyst was heated to 698 K and then exposed to a flowing mixture with 10% O_2 and 90% He, flushed with He, and finally reduced in a flowing mixture of 10% H_2 and 90% He. The sample was then flushed with He and cooled to room temperature under He flow. To produce the oxidized sample, the catalyst was heated to 698 K under a flow of 10% O_2 and 90% He, cooled to 423 K in flowing He, and exposed to the 10% H_2 and 90% He mixture at this temperature to reduce the PdO to Pd. After flushing with He, the sample was cooled to room temperature. To measure the spectrum of adsorbed CO, a 10% CO−90% He mixture was passed over the catalyst at room temperature before flushing it with flowing He and acquiring the spectra at room temperature under He flow.

The reducibility of the $Pd@CeO_2/Al_2O_3$ catalyst under reaction conditions was determined using a flow-titration/temperature-programmed-oxidation (TPO) system that is described in more detail elsewhere.[11] In these experiments, 0.5 g of sample were placed in a tubular reactor, exposed to various environments, and then purged with dry He for 30 min. The oxidation states of the catalysts were then determined by reoxidizing the samples in flowing air (21% O_2 and 79% N_2 at 3.0 mL min^{-1}) while monitoring the effluent gases using a quadrupole mass spectrometer. Oxygen consumption was determined by comparing the lag in the O_2 signal and the N_2 signal.

TABLE 1: Textural Properties of the Bare Al_2O_3 Support and the $Pd(1\%)@CeO_2(9\%)/Al_2O_3$ Catalyst

sample	surface area (m^2 g^{-1})	total pore volume (mL g^{-1})	D_{MAX} (nm)[a]
Al_2O_3	91	0.94	40
$Pd(1\%)@CeO_2(9\%)/Al_2O_3$	93	0.69	40

[a] Maximum of the pore distribution taken from the desorption branch.

3. Results and Discussion

The physical characteristics of the alumina support and the $Pd@CeO_2/Al_2O_3$ are summarized in Table 1. The alumina used for the support had a relatively low BET surface area of 91 m^2/g, with large pores ranging up to 40 nm in diameter. Due to the low loading of $Pd@CeO_2$, the surface area and pore-size distribution of the $Pd@CeO_2/Al_2O_3$ catalyst were similar to that of the alumina support. The only difference between the bare support and the final catalyst is that the volume of the pores decreased following impregnation with $Pd@CeO_2$. XRD data (not shown) of the $Pd@CeO_2/Al_2O_3$ showed peaks associated with the fluorite structure of crystalline ceria, in addition to reflections attributable to the alumina support. Using Scherrer's equation and the width of the (111) reflection, the crystallite size of the ceria was 3 nm. This is similar to the dimension of CeO_2 shell of the starting $Pd@CeO_2$ particles observed by HRTEM.[10] No reflections associated with Pd were found due to the low Pd loading and the small size of the Pd particles (<2 nm).

The initial rates for the WGS reaction over the oxidized $Pd@CeO_2/Al_2O_3$ were very similar to those reported earlier for a conventional, 1 wt % Pd, 99 wt % ceria catalyst.[12] At 623 K in 25 Torr each of CO and H_2O, the reaction rate was 3×10^{18} molecules/s g; however, the rates declined dramatically with time over the period of 1 h. As shown in Figure 1, the initial conversion of CO was 12% but this decreased to 4% after 60 min. This decrease in activity could be completely reversed by oxidizing the catalyst in flowing air at 623 K for a few minutes, suggesting that the change in catalytic activity is related to reduction of the catalyst in the WGS environment. Although not shown in Figure 1, the conversion of H_2O followed the conversion of CO within experimental uncertainty.

It is easily demonstrated that the transient CO conversion in Figure 1 is not simply due to reduction of the catalyst. In addition to the fact that H_2O conversion followed CO conversion, the amount of oxygen in the catalyst is negligible compared to the amount of CO_2 produced over the 60-min period in Figure 1. Because the mass of catalyst used in this particular experiment was 80 mg, complete reduction of PdO to Pd and CeO_2 to Ce_2O_3 would yield a maximum of 30 μmol of CO_2. By comparison, approximately 1000 μmol of CO_2 were formed during the course of a deactivation cycle in Figure 1.

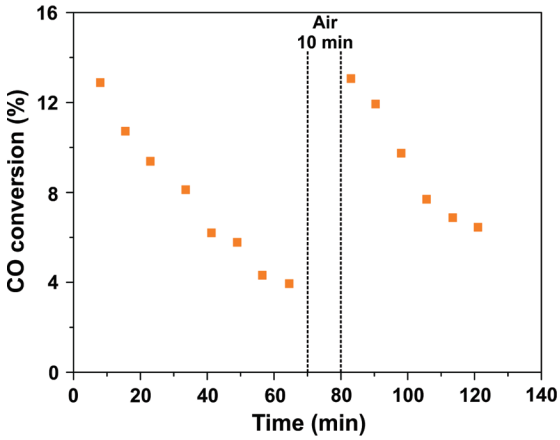

Figure 1. Evolution of CO conversion during the WGS reaction at 623 K over the $Pd@CeO_2/Al_2O_3$ catalyst.

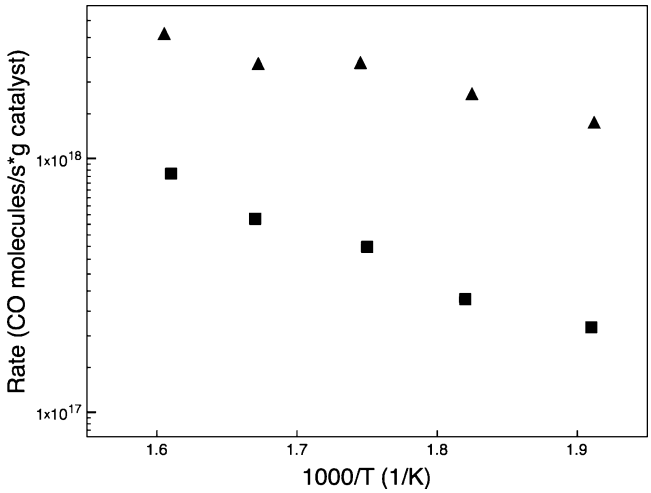

Figure 2. Reaction rates for the WGS reaction over the $Pd@CeO_2/Al_2O_3$ catalyst for samples freshly oxidized in air at 623 K (▲) and reduced in H_2 at 623 K (■).

The WGS reaction rates for the $Pd@CeO_2/Al_2O_3$ catalyst as a function of temperature are shown in Figure 2. Two measurements were performed at each temperature; the initial rate for a catalyst that was freshly oxidized in air at 623 K, and the rate for a sample reduced in H_2 at 623 K. The activation energy of the reduced sample, 38 kJ/mol, was found to be similar to conventional Pd/CeO_2 catalysts[12] and somewhat greater than that of the oxidized sample (21 kJ/mol).

It is interesting to compare the reaction behavior in Figure 1 to that of more conventional Pd/ceria catalysts. In contrast to the results for $Pd@CeO_2/Al_2O_3$, conventional Pd/ceria catalysts exhibit stable WGS activity for periods of many hours. The slow deactivation which has been observed with ceria-supported metals under steady-state, WGS conditions appears to be due to sintering of the metal and cannot be reversed by simple oxidation.[3,4] Indeed, thermodynamic data for bulk ceria indicates that ceria should not be reduced by the WGS environment and that the O:Ce ratio should be very close to 2.[16] The rapid deactivation in Figure 1 is remarkably similar to what has been reported for Pd catalysts supported on praseodymia and ceria-praseodymia solid solutions.[12] Praseodymia exhibits chemistry similar to that of ceria but is much more easily reduced. It is oxidized to PrO_2 only with great difficulty[17] and is found to exist as Pr_2O_3 under WGS conditions,[12] in agreement with thermodynamic data for the bulk compound.[18]

To understand how the redox properties of the $Pd@CeO_2/Al_2O_3$ catalyst differ from that of a conventional Pd/ceria catalyst, we measured the oxidation states of the $Pd@CeO_2/Al_2O_3$ after various pretreatments using flow titration, with the results reported in Table 2. In these experiments, the sample was exposed to different gaseous environments at 623 K, and then the amounts of O_2 taken up by the sample upon exposure to air at 623 K were measured. Reduction in dry, flowing H_2 led to significant reduction, so that 200 μmol of O/g of sample was required for reoxidation. If all of this were associated with the ceria component, the O:Ce ratio of the reduced $Pd@CeO_2/Al_2O_3$ would be approximately 1.61. Since as much as half of the oxygen uptake could be due to oxidation of Pd to PdO, the O:Ce ratio in the ceria component of the catalyst could be as high as 1.80, a value similar to that reported in similar experiments performed on a conventional Pd/ceria catalyst.[12] Unfortunately, it is difficult to separate reduction of Pd from that of ceria, since reduction of both species occur simultaneously in commonly employed techniques such as TPR.[9,19]

TABLE 2: Oxygen Consumption by the $Pd@CeO_2/Al_2O_3$ Catalyst Following Reduction by Pure H_2 Gas at 623 K, Oxidation in Air at 623 K Followed by Exposure to WGS Conditions at 623 K, and Reduction in H_2 with Subsequent Partial Oxidation by 25 Torr H_2O at 623 K

pretreatment	oxygen uptake (μmol O/g catalyst)	O:Ce ratio
H_2	200	1.61
air, followed by WGS	150	1.70
H_2, followed by steam	180	1.66

The results obtained following exposure of the $Pd@CeO_2/Al_2O_3$ to the WGS environment at 623 K are more significant. Following reaction in 25 Torr each of CO and H_2O, 150 μmol of O/g was taken up by the catalyst, indicating the O:Ce ratio of the working catalyst is 1.70. By comparison, a traditional Pd/ceria catalyst remained essentially oxidized following this pretreatment.[12] The implication is that CO and H_2 are more effective in reducing the $Pd@CeO_2/Al_2O_3$ catalyst than H_2O and CO_2 are in oxidizing it. To further test this idea, we reduced the $Pd@CeO_2/Al_2O_3$ catalyst in dry H_2 at 623 K and then passed 25 Torr of H_2O (in He) over the catalyst for 0.5 h at 623 K before measuring the amount of oxygen that could be consumed by the catalyst. As expected, the catalyst was not significantly reoxidized by the steam, requiring 180 μmol of O/g (O:Ce ratio of 1.66) to complete the reoxidation process in air at 623 K. A similar experiment with a traditional Pd/ceria catalyst found that steam was very efficient in reoxidizing the ceria.[12]

The data in Table 2 suggest that the redox properties of the ceria in the shell of the $Pd@CeO_2/Al_2O_3$ catalyst are very different from that of bulk ceria, with the ceria in the shell being much more easily reduced. While we cannot provide a definitive explanation for why the ceria shell is more reducible, it is noteworthy that neutron-scattering experiments have shown that reducible forms of ceria have a different average local structure on the atomic scale, as quantified by their pair-distribution functions.[19] The local fluorite structure in CeO_2 is critical for stabilizing Ce(IV),[20] a fact highlighted by the observation that Ce(III) is the more stable species in many other environments, such as in $CeVO_4$.[20−22] Therefore, we suggest that the Pd particle may act as a template for the growth of the ceria shell in $Pd@CeO_2$, resulting in a more locally disordered form of ceria with less ability to stabilize Ce(IV).

An important question about $Pd@CeO_2$ catalysts concerns the accessibility of the Pd. In conventional Pd/ceria catalysts, WGS activity has been shown to increase linearly with surface Pd,[3,4] demonstrating that the active sites are associated with Pd.

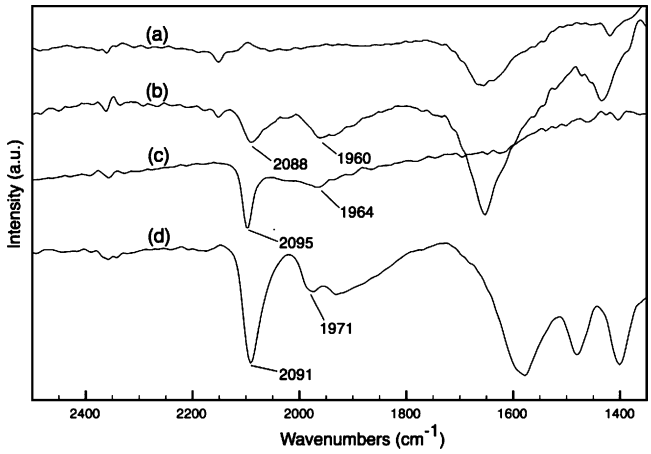

Figure 3. Diffuse reflectance FTIR spectra of $Pd@CeO_2/Al_2O_3$ nanocomposite after, reduction at 698 K followed by exposure to CO at room temperature (a), oxidation at 698 K followed by exposure to CO at room temperature (b), Pd nanoparticles deposited on alumina after reduction at 698 K followed by exposure to CO at room temperature (c), and a conventional 1% Pd/ceria catalyst after reduction at 698 K followed by exposure to CO at room temperature.

However, several recent investigations of WGS activity using noble metal/ceria core−shell catalysts have reported high activities and low CO uptakes.[8,23,24] The authors suggested that the active sites for WGS reside on the metal-promoted ceria shell, rather than on the metal surface itself.

Our initial attempts to measure CO adsorption on a $Pd@CeO_2/Al_2O_3$ sample that had been prereduced in H_2 also showed a complete absence of CO adsorption at room temperature. However, since the high initial WGS rates appear to be associated with an oxidized catalyst, we performed additional experiments that would allow us to look for CO adsorption on oxidized samples. First, a series of FTIR experiments were performed with different pretreatments of the catalyst, with results shown in Figure 3. The spectrum in Figure 3a was taken on the $Pd@CeO_2/Al_2O_3$ catalyst following pretreatment similar to those used in the room-temperature CO adsorption measurements. The sample was oxidized, reduced under a flow of 10% H_2−He at 700 K, exposed to CO at room temperature, and then flushed with dry He at room temperature. Bands corresponding to adsorbed CO are not observed, in agreement with the CO uptake measurements. To mimic the initial oxidized state of the catalyst during the WGS studies, the $Pd@CeO_2/Al_2O_3$ was oxidized at 700 K and then subjected to a very mild reduction in 10% H_2−He at 473 K before exposure to CO at room temperature. Bands associated with terminal (2088 cm^{-1}) and bridging (1960 cm^{-1}) CO on Pd are clearly visible in Figure 3b, confirming that the Pd particles are able to adsorb CO. Bands observed at 1435 and 1655 cm^{-1} are likely due to carbonate species[25] and adsorbed water, respectively. For comparison, spectra following room-temperature adsorption of CO onto a Pd/Al_2O_3 sample obtained by deposition of MUA-Pd nanoparticles onto alumina (Figure 3c) and a conventional 1 wt % Pd/ceria catalyst (Figure 3d) are also shown. The peak frequencies associated with CO adsorption on the Pd in these two samples are essentially the same as on the oxidized $Pd@CeO_2/Al_2O_3$, confirming that adsorption on the oxidized $Pd@CeO_2/Al_2O_3$ is associated with the Pd.

As further confirmation that the metal is accessible in the case of an oxidized catalyst, CO adsorption measurements were performed also on the oxidized catalyst using the procedure described in the Experimental Methods. Again, the oxidized catalyst was reduced in H_2 at 473 K to reduce the Pd without reducing the ceria. CO adsorption then carried out at 195 K, a temperature that has been shown to be sufficiently low so as to avoid reaction with ceria. Using this approach, the Pd dispersion was calculated to be 11%.

It is interesting to ask why a reduced ceria shell leads to the suppression of CO adsorption in $Pd@CeO_2$ catalysts. Although it is tempting to associate adsorption suppression with electron-transfer effects, such as were originally used to explain strong metal support effects (SMSI) with titania-supported catalysts,[26] SMSI associated with titania is now generally acknowledged to be due to migration of a reduced titania over the metal particles.[27] Although this generally occurs under more severe reducing conditions (e.g., higher temperature) than employed in our experiments, the ceria in the $Pd@CeO_2/Al_2O_3$ composites appears to be highly reducible. HRTEM experiments performed on conventional precious metal/ceria materials were unable to detect decoration or migration effects on ceria that was reduced at moderate temperatures even if this treatment was able to suppress CO or H_2 chemisorption, leading the authors of those studies to suggest that adsorption suppression was associated with an electron-transfer effects.[28−31] However, the presence of a very thin reduced layer of reduced ceria decorating metal nanoparticles cannot be fully excluded by HRTEM. Indeed, Pan and co-workers recently described HRTEM evidence for partial encapsulation of Pd particles by reduced ceria-zirconia.[32]

In the $Pd@CeO_2/Al_2O_3$ catalyst of our study, a ceria overlayer clearly is present. The question is simply why does this overlayer effectively block adsorption only when it is reduced. We propose an alternative explanation to electron-transfer effects, shown diagrammatically in Figure 4. In this picture, the oxidized CeO_2 forms a shell with many cracks and fissures that allow gases to approach the Pd core. However, when CeO_2 is reduced, these fissures close. This effect may be either due to the decreased

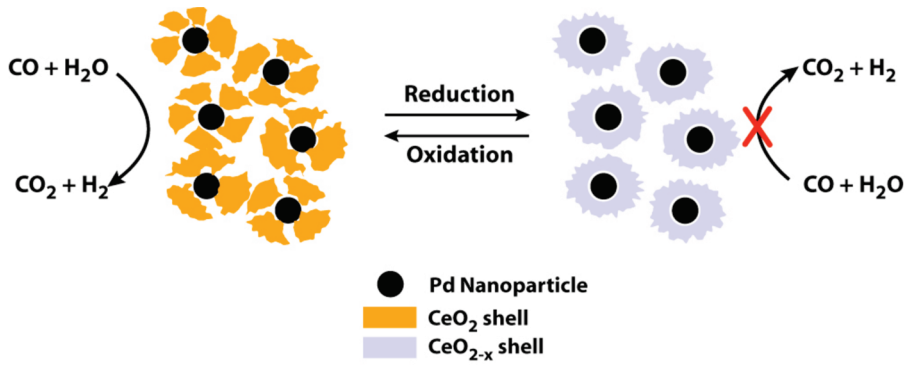

Figure 4. Schematic representation of changes in shell morphology for oxidized and reduced catalyst.

density of Ce_2O_3 or because the reduced ceria may also interact more strongly with the Pd, spreading out to more effectively block the Pd from adsorbing CO. In general, "SMSI-like" effects are associated with reducible supports, and the enhanced reducibility of the ceria shell in the $Pd@CeO_2/Al_2O_3$ catalyst compared to bulk ceria may in part explain why these effects appear to be significant at mild conditions. Furthermore, the core−shell structure of the catalyst, which is expected to have a high contact area between Pd and ceria, may also result in an increased tendency for ceria to spread out onto the Pd.

At this time, we cannot determine which effect is most important in causing deactivation of the $Pd@CeO_2/Al_2O_3$ catalyst: the CO adsorption suppression or the low oxygen content of the ceria at steady-state. We know from the case of the praseodymia-supported catalysts that the inability of the support to be oxidized by steam can result in low rates for the WGS reaction.[12] Likewise, WGS rates on Pd/ceria catalysts have been shown to increase linearly with CO adsorption uptakes.[3] Therefore, both of these effects are likely contributors to the deactivation that was observed.

While the properties of $Pd@CeO_2/Al_2O_3$ that we prepared are not ideal for WGS, they are clearly different from that of conventional Pd/ceria catalysts. The ease with which the ceria shell is reduced, the intimate contact between the Pd and the ceria, and special isolation of the Pd by the ceria shell may well allow materials of this type to find applications where reduction of the ceria shell does not cause deactivation.

4. Conclusions

The results in this study demonstrate that $Pd@CeO_2$ can exhibit catalytic properties that are dramatically different from that of conventional Pd/ceria. The ceria in the core−shell catalysts exhibits different redox properties from those found for the ceria in conventional catalysts, possibly due to structural changes associated with the Pd-core template. Even when the Pd in the oxidized catalysts is accessible to gas-phase reactants, reduction of the ceria can cause encapsulation of the Pd, which can in turn lead to deactivation of the catalyst for reactions like water-gas shift. Clearly, the properties of these materials are unique and their application will require proper consideration of those properties.

Acknowledgment. Professor Mauro Graziani (University of Trieste) is acknowledged for stimulating helpful discussions. R.J.G., N.W., and K.B. acknowledge support from AFOSR (MURI), Grant No. FA9550-08-1-0309. M.C., T.M., and P.F. acknowledge the University of Trieste, ICCOM-CNR, INSTM and PRIN2007 "Sustainable processes of 2nd generation for the production of H_2 from renewable resources" for financial support.

References and Notes

(1) Gorte, R. J.; Zhao, S. *Catal. Today* **2005**, *104*, 18–24.
(2) Trovarelli, A. *Catal. Rev. Sci. Eng.* **1996**, *38*, 439–520.
(3) Wang, X.; Gorte, R. J.; Wagner, J. P. *J. Catal.* **2002**, *212*, 225–230.
(4) Ruettinger, W.; Liu, X. S.; Farrauto, R. J. *Appl. Catal., B* **2006**, *65*, 135–141.
(5) Budroni, G.; Corma, A. *Angew. Chem., Int. Ed.* **2006**, *45*, 3328–3331.
(6) Budroni, G.; Corma, A.; Garia, H.; Primo, A. *J. Catal.* **2007**, *251*, 345–353.
(7) De Rogatis, L.; Cargnello, M.; Gombac, V.; Lorenzut, B.; Montini, T.; Fornasiero, P. *ChemSusChem* **2010**, *3*, 24–42.
(8) Yeung, C. M. Y.; Tsang, S. C. *Catal. Lett.* **2009**, *128*, 349–355.
(9) Cargnello, M.; Montini, T.; Polizzi, S.; Wieder, N. L.; Gorte, R. J.; Graziani, M.; Fornasiero, P. *Dalton Trans.* **2010**, *39*, 2122.
(10) Cargnello, M.; Wieder, N. L.; Montini, T.; Gorte, R. J.; Fornasiero, P. *J. Am. Chem. Soc.* **2009**, *132*, 1402–1409.
(11) Kim, T.; Vohs, J. M.; Gorte, R. J. *Ind. Eng. Chem. Res.* **2006**, *45*, 5561–5565.
(12) Bakhmutsky, K.; Zhou, G.; Timothy, S.; Gorte, R. J. *Catal. Lett.* **2009**, *129*, 61–65.
(13) Hilaire, S.; Wang, X.; Luo, T.; Gorte, R. J.; Wagner, J. *Appl. Catal., A* **2001**, *215*, 271–278.
(14) Sharma, S.; Hilaire, S.; Vohs, J. M.; Gorte, R. J.; Jen, H. W. *J. Catal.* **2000**, *190*, 199–204.
(15) Tanabe, T.; Nagai, Y.; Hirabayashi, T.; Takagi, N.; Dohmae, K.; Takahashi, N.; Matsumoto, S. i.; Shinjoh, H.; Kondo, J. N.; Schouten, J. C.; Brongersma, H. H. *Appl. Catal., A* **2009**, *370*, 108–113.
(16) Zhou, G.; Hanson, J.; Gorte, R. J. *Appl. Catal., A* **2008**, *335*, 153–158.
(17) Putna, E. S.; Vohs, J. M.; Gorte, R. J.; Graham, G. W. *Catal. Lett.* **1998**, *54*, 17–21.
(18) Zhou, G.; Gorte, R. J. *J. Phys. Chem. B* **2008**, *112*, 9869–9875.
(19) Mamontov, E.; Egami, T. *J. Phys. Chem. Solids* **2000**, *61*, 1345–1356.
(20) Da Silva, J. L. F.; Ganduglia-Pirovano, M. V.; Sauer, J. *Phys. Rev. B* **2007**, *76*, 125117.
(21) Reidy, R. F.; Swider, K. E. *J. Am. Ceram. Soc.* **1995**, *78*, 1121–1122.
(22) Shah, P. R.; Khader, M. M.; Vohs, J. M.; Gorte, R. J. *J. Phys. Chem. C* **2008**, *112*, 2613–2617.
(23) Yeung, C. M. Y.; Tsang, S. C. *J. Phys. Chem. C* **2009**, *113*, 6074–6087.
(24) Yeung, C. M. Y.; Yu, K. M. K.; Fu, Q. J.; Thompsett, D.; Petch, M. I.; Tsang, S. C. *J. Am. Chem. Soc.* **2005**, *127*, 18010–18011.
(25) Zhao, S.; Gorte, R. J. *Appl. Catal., A* **2004**, *277*, 129–136.
(26) Tauster, S. J.; Fung, S. C.; Baker, R. T. K.; Horsley, J. A. *Science* **1981**, *211*, 1121–1125.
(27) Roberts, S.; Gorte, R. J. *J. Catal.* **1990**, *124*, 553–556.
(28) Sa, J.; Bernardi, J.; Anderson, J. A. *Catal. Lett.* **2007**, *114*, 91–95.
(29) Bernal, S.; Calvino, J. J.; Cauqui, M. A.; Gatica, J. M.; Larese, C.; Omil, J. A. P.; Pintado, J. M. *Catal. Today* **1999**, *50*, 175–206.
(30) Gatica, J. M.; Baker, R. T.; Fornasiero, P.; Bernal, S.; Kaspar, J. *J. Phys. Chem. B* **2001**, *105*, 1191–1199.
(31) Feio, L. S. F.; Hori, C. E.; Damyanova, S.; Noronha, F. B.; Cassinelli, W. H.; Marques, C. M. P.; Bueno, J. M. C. *Appl. Catal., A* **2007**, *316*, 107–116.
(32) Sun, H. P.; Pan, X. P.; Graham, G. W.; Jen, H. W.; McCabe, R. W.; Thevuthasan, S.; Peden, C. H. F. *Appl. Phys. Lett.* **2005**, *87*, 201915-.

JP102965E